ADVANCED FUNCTIONAL MATERIALS
www.afm-journal.de

Liquid Metal Marbles

Vijay Sivan, Shi-Yang Tang, Anthony P. O'Mullane, Phred Petersen, Nicky Eshtiaghi, Kourosh Kalantar-zadeh, and Arnan Mitchell**

Liquid metal marbles that are droplets of liquid metal encapsulated by micro- or nanoparticles are introduced. Droplets of galinstan liquid metal are coated with insulators (including Teflon and silica) and semiconductors (including WO_3, TiO_2, MoO_3, In_2O_3 and carbon nanotubes) by rolling over a powder bed and also by submerging in colloidal suspensions. It is shown that these marbles can be split and merged, can be suspended on water, and are even stable when moving under the force of gravity and impacting a flat solid surface. Furthermore, the marble coating can operate as an active electronic junction and the nanomaterial coated liquid metal marble can act as a highly sensitive electrochemical based heavy metal ion sensor. This new element thus represents a significant platform for the advancement of research into soft electronics.

1. Introduction

The term "liquid marble" was first introduced nearly a decade ago to describe droplets of aqueous fluid encapsulated within hydrophobic particles.[1] These liquid marbles behave, to some degree, like solid particles, but due to the fact that their structural form is dominated by surface tension, they exhibit a number of unique properties, including very small contact area with surfaces leading to low friction rolling, superhydrophobic interactions with other fluids and the ability to be split or fused together with self-healing encapsulation layers.[2] Liquid marbles rely on surface tension and can be formed with both non-polar or polar fluids including water.[1–5] Indeed, water solutions encased with hydrophobic particles have great potential for encapsulating biological environments even at nanolitre scales.[6] Due to the unique properties of liquid marbles, there has been significant research effort invested in establishing their capabilities and exploring practical applications.[7–10]

Liquid metals have a long history of study in the fields of analytical chemistry, electronics, and experimental physics. Traditionally, the most common liquid metal to be studied has been mercury.[11] The toxicity of mercury however rendered applications based on this liquid metal unattractive and thus research interest into the applications of liquid mercury has remained a niche area. Recently, less hazardous liquid metals including eutectic alloys of gallium (75%) and indium (25%) (eGaIn);[12,13] and of gallium (68.5%), indium (21.5%) and tin (10%), (Galinstan)[11,14,15] have become readily available and thus research interest in these alternative liquid metals is gaining momentum. In general, liquid metals offer several unique properties including high density (6440 kg/m^3 [11]), high surface tension (534.6 ± 10.7 mN/m[14]) and extremely low vapor pressure (<10^{-6} Pa at 500 °C[11]) allowing them to operate as liquids under vacuum conditions and at high temperatures.[11] Most importantly, liquid metals offer the highest conductivity of any liquids, with orders of magnitude less resistive loss than ionic fluids making them attractive for various applications, such as in soft electronic components,[12,13] stretchable antennas,[16–18] interconnects,[19,20] electromagnets,[21] MEMS switches[22] and reconfigurable wires.[23]

Despite these many desirable properties, liquid metals share one major disadvantage for practical use in that they are highly corrosive, particularly to other metals.[24] This means that they will dissolve and amalgamate with solid contact metals such as gold which would be typically used to electrically interface to the liquid metal to exploit its properties. Liquid metals based on eutectic alloys of gallium in ambient air, forms a thin oxide layer which will also adhere strongly to ionic surfaces such as glass[11,14,25] and even relatively low surface energy polymers including polydimethylsiloxane (PDMS) which is often used to manipulate fluids.[22] In order to effectively exploit the attractive properties of liquid metals, a means must be found to prevent the fluid metal from adhering to its environment or corroding its metal contacts, while maintaining both the flexible re-configurability offered by the fluid and access to the electronic properties of the liquid metal.

Dr. V. Sivan, S.-Y. Tang, Prof. K. Kalantar-zadeh
School of Electrical and Computer Engineering
RMIT University
GPO Box 2476, Melbourne VIC 3001, Australia
E-mail: kourosh.kalantar@rmit.edu.au
Dr. A. P. O'Mullane
School of Applied Sciences
RMIT University
GPO Box 2476, Melbourne VIC 3001, Australia
P. Petersen
School of Media and Communication
RMIT University
GPO Box 2476, Melbourne VIC 3001, Australia
Dr. N. Eshtiaghi
School of Civil, Environmental and Chemical Engineering
RMIT University
GPO Box 2476, Melbourne, VIC 3001, Australia
Prof. A. Mitchell
Centre for Ultra-high bandwidth Devices for Optical Systems (CUDOS)
School of Electrical and Computer Engineering
RMIT University
GPO Box 2476, Melbourne VIC 3001, Australia
E-mail: arnan.mitchell@rmit.edu.au

DOI: 10.1002/adfm.201200837

In this paper, we present a novel approach to the use of liquid metals through the creation of liquid metal marbles. Here we encapsulate small droplets of galinstan within a coating of nanoscale powders. We comprehensively studied the physical properties of such liquid metal marbles in terms of their splitting and fusing upon applying a force, floating on aqueous media and dynamic properties during their free fall and impact on hydrophobic and hydrophilic surfaces. We show that powders of nanoparticles can be used to achieve liquid metal marbles with semiconducting properties at their surface. Achieving this, we demonstrate several liquid metal marble capabilities including the formation of metal-semiconductor-metal (MSM) soft electronic devices and investigate their *I–V* transfer characteristics. Finally, we demonstrate the utility of this new liquid metal marble through its use as a highly sensitive and selective heavy metal ion sensor.

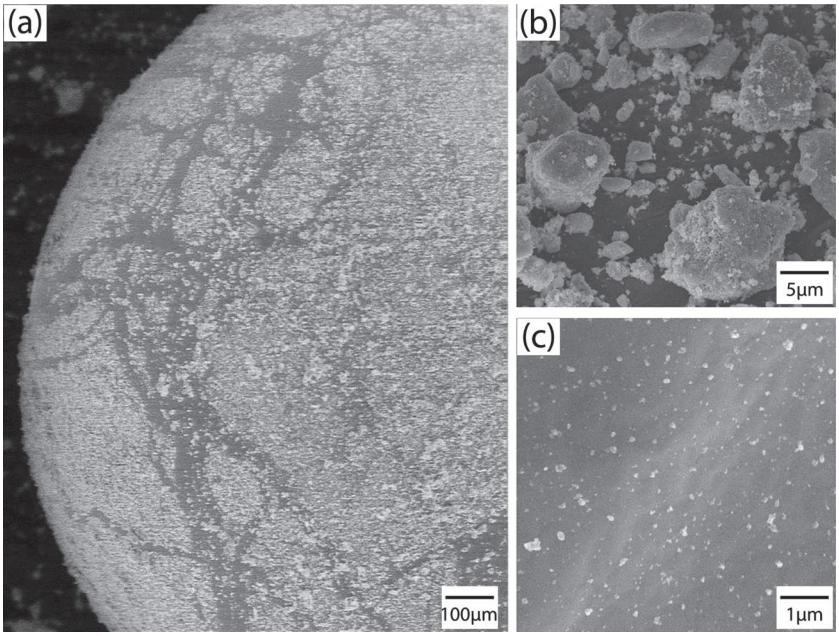

Figure 1. SEM images of a liquid metal marble: a,b) galinstan droplet encapsulated in a coating of 80 nm WO_3 nanoparticles by rolling it on a powder bed and c) surface of the liquid metal marble formed by submerging a liquid metal droplet in a colloidal dispersion of 0.7 g of WO_3 nanoparticles in 50 ml DI water.

2. Realization of Liquid Metal Marbles

Liquid marbles are typically realized by rolling a small aqueous droplet over a bed of powder to achieve a uniform coating.[1] For aqueous droplets, the powder coating must be hydrophobic, such that the surface tension prevents the particles from sinking into the fluid.[1] The exceptionally strong cohesive forces between the alloyed liquid metal elements results in a contact angle of greater than 90° being observed when liquid metal droplets rest on almost all non-metallic material surfaces. Thus, most non-metals are considered as 'phobic' to the liquid metal. This greatly expands the range of powder materials that do not sink or amalgamate into the liquid metal and can be used as liquid marble coatings.

In this paper, we report on the realization and application of liquid marbles formed from the liquid metal galinstan, (a eutectic alloy of Ga, In and Sn). We have adapted two methods for coating the liquid metal with powder: a) rolling the droplet on a powder bed and b) submerging the liquid metal droplet in a colloidal suspension of micro- or nanopartices. **Figure 1** presents scanning electron microscopy (SEM) images of liquid metal marbles formed using these techniques. Figure 1a,b present images of liquid metal marbles formed by rolling a droplet of galinstan on a powder bed of WO_3 nanoparticles (particle size ca. 80 nm). Here it can be seen that the coating is not uniform and consists of multiple layers of particles. Tears evident in the coating are due to the expansion of the liquid metal marble when imaged under vacuum in the SEM. In a traditional liquid marble, such tears would 'heal' due to the redistribution of the particles on the surface. It has been previously reported that any exposed region of the galinstan alloy to air or even as little as 0.2% volume of oxygen will cause a thin, solid film of gallium oxide to form at the surface.[14] We expect that such a film should be present on the galinstan marbles which would prevent the free movement of particles on the surface. This would explain the tears observed in Figure 1a.

Figure 1c shows the surface of a liquid metal marble formed by submerging a galinstan droplet in a suspension of the same 80 nm WO_3 nanoparticles in DI water (0.7g WO_3: 50 ml DI water). A sparse, but uniform coating is observed. If the concentration of particles in the suspension is increased, the density of the coating can also be increased (Supporting Information S1), demonstrating that submersion in a suspension allows control of the loading of the particles on the surface. The sparsely coated marbles can be rolled on a normally wetting surface (such as Si) without it adhering to the surface (Supporting Information S2). We believe that this is the first reported use of immersion in a colloidal suspension to form liquid marbles and further anticipate that this technique could be extended to the encapsulation of any immiscible droplets in aqueous media.

Our observations have shown that suitable powders include typical low-surface energy materials such as Teflon, but extend to polar insulators such as SiO_2 and even semiconductors such as ZnO and WO_3 and conducting carbon nanotubes. SEM images of the surface coverage achievable with some of these powder materials are presented in **Figure 2**.

3. Physical Properties

Liquid marbles are attractive due to their many unique physical properties, which include a large contact angle and hence low rolling friction; the ability to be split into smaller marbles or merged together; the ability to rest on the surface of various liquids supported by surface tension; and the ability to remain stable under impact.[2] In the following we report on a number

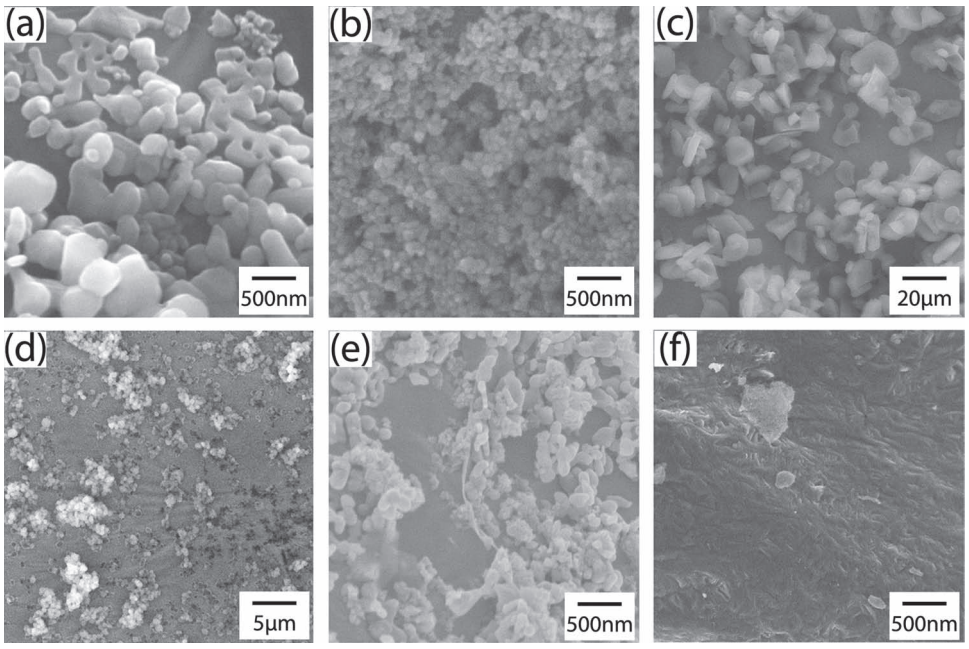

Figure 2. SEM images of different powders that are coated on the surface of galinstan by rolling on a powder bed: a) ZnO nanoparticles(≈100 nm), b) In_2O_3 nanoparticles (≈30 nm), c) Al_2O_3 powder (≈9 μm), d) Teflon powder (≈1 μm), e) TiO_2 nanoparticles (≈100 nm), and f) single wall carbon nanotubes (≈1 nm diameter and lengths of several micrometers).

of investigations to determine whether liquid metal marbles also possess such properties. It is anticipated that the thin oxide layer formed when galinstan is exposed to air would significantly effect the observed properties. To establish the effect of this oxide, many of the experiments have been conducted with this oxide present and then repeated after treating the galinstan with diluted HCl solution (6%),[26] before coating the droplet with the powder to eliminate the oxide layer. Firstly, in **Figure 3**a we present the shape of the galinstan droplet with the naturally formed oxide layer resting on wetting (silicon) and non-wetting (Teflon) surfaces. The tips formed from the dispensing of the droplet do not relax and can be observed. This is attributed to the oxidation of the surface of galinstan.[14] When the droplets were treated with diluted HCl solution to reduce the oxide layer, the tip relaxes and a spherical shape is achieved as has been previously reported.[26] Lastly, we present the coated (rolled on 80 nm WO_3 powder bed) droplets of galinstan resting on wetting and non-wetting surfaces. The coated droplets possess the characteristics similar to those of liquid marbles and do not adher to the surfaces.

To test the ability to merge and split the liquid metal marbles, we formed two marbles by rolling HCl treated galinstan droplets on 80 nm WO_3 powder bed, placed them in close proximity and mechanically pressed them together. Figure 3b presents a photograph of the original separate droplets, the application of a spatula to press the marbles together, and the resulting fused marble. The final marble is relatively large and is quite spherical in shape. To demonstrate splitting, a single liquid metal marble was formed by rolling an HCl treated galinstan droplet on an 80 nm WO_3 powder bed and then was cut using a scalpel. Figure 3c presents photographs of the original marble, cutting with a scalpel blade and the resulting pair of marbles.

To test whether a liquid metal marble coated with hydrophobic particles can be suspended on the surface of water due to surface tension, we rolled a galinstan droplet on a powder bed of Al_2O_3 powder treated with Sigmacote to render it hydrophobic. We then placed the droplet on the surface of a beaker of water. Figure 3d shows this coated droplet suspended on the surface of water. Significant displacement of the water is evident due to the considerable weight of the liquid metal marble.

To test the behavior of liquid metal marbles under impact after free fall, we compared the behavior of an uncoated droplet of galinstan to a liquid metal marble (galinstan, with native oxide intact, rolled on 80nm WO_3 powder bed) after release from a height of 25 mm and impacting on a silicon surface. A high speed camera (1600 images per second) was used to record the image of the droplets during the fall and impact.

Figure 4a presents sequential images of the uncoated galinstan after being dispensed from a pipette, falling and impacting on a Si surface. The droplet maintains a teardrop shape throughout the free fall. This shape is maintained due to the oxide skin that is naturally formed on the surface of the liquid metal droplet in ambient conditions. At the impact, a crown-like rim having an obtuse contact angle is observed, transforming into one with its angle of contact receding to an acute angle and is quickly transformed from a pendant shape to a more even conical shape. No rebound from the surface is observed. The free fall and impact video can been seen in the Supporting Information Video SV1.

Figure 4b shows the coated galinstan liquid marble fall, after being released from a spatula, and impacting on the same surface. The marble retains its almost spherical shape during

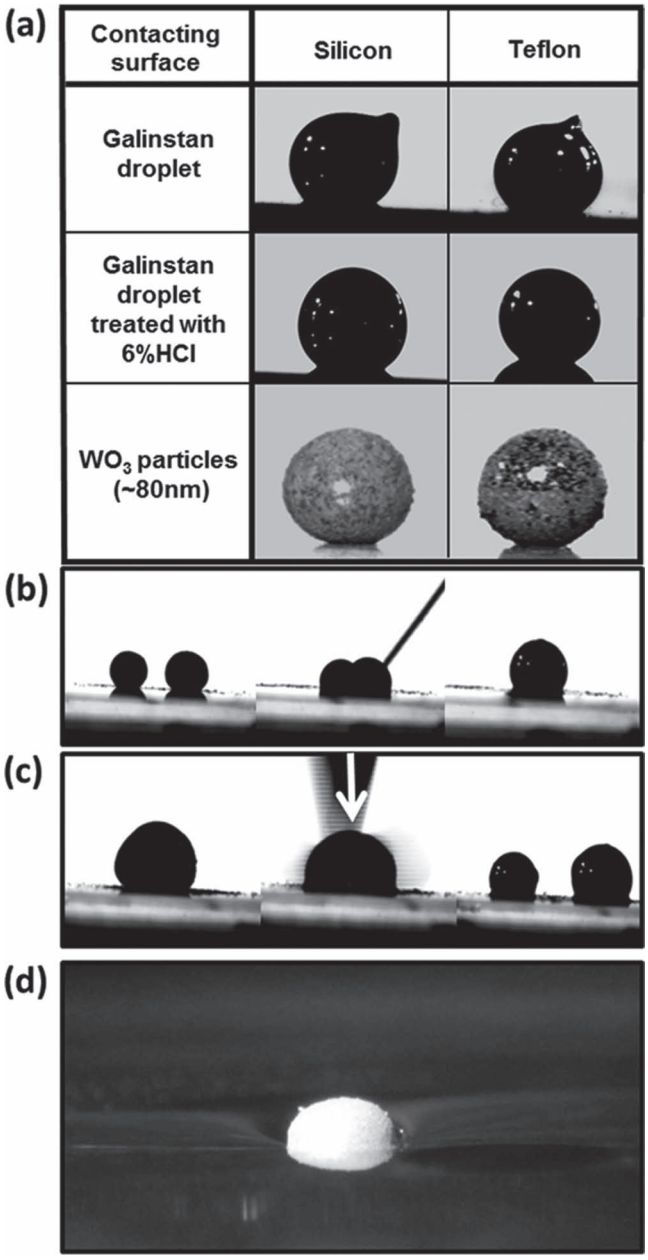

Figure 3. Physical properties of liquid metal marbles. a) Images of a galinstan droplet with naturally formed native oxide layer in ambient air, a galinstan droplet treated with diluted HCl solution and WO_3 powder coated galinstan on a wetting (Si) and non-wetting (Teflon) surface. WO_3 powder was used to coat the galinstan droplet by rolling it on a powder bed. b) Merging of two diluted HCl solution treated WO_3 powder (≈80 nm) coated galinstan droplets. A spatula was used to provide the external mechanical force. c) A diluted HCl solution treated WO_3 powder (≈80 nm) galinstan droplet was cut using a scalpel blade to realize two separate galinstan coated droplets. d) Sigmacote treated Al_2O_3 powder (≈9 μm) coated galinstan droplet floating on water.

its free fall. At the impact, a crown-like rim is again observed having an obtuse contact angle. Interestingly, we also observed significant tears on the coated surface together with the shedding of some of the particles at impact (clearly seen in the Supporting Information Video SV2). The tears are likely due to the presence of the native oxide as HCl treatment was not performed in this experiment, and appear to close up and the marble is observed to regain its almost spherical shape as it rebounds from the surface. This is a characteristic that is not seen to the same extent in conventional aqueous liquid marbles. Figure 4c is the zoomed in photographs of the last three frames of Figure 4b showing the rebound of the galinstan marble from the surface and its return. This characteristic can be more clearly seen in the Supporting Information Video SV2. Upon return to the surface the marble rolls freely on the surface and behaves like a true liquid marble.

4. Electronic Properties

An important property of the liquid metal droplets is the high electrical conductivity of the liquid metal itself. The use of uncoated liquid metal for so called 'soft electronics' has been reported previously,[12,13] however, the corrosive nature of the liquid metal in contact with other metals imposes certain limitations. Our finding that liquid metals can be encapsulated within semiconducting and insulating coatings presents new opportunities for the realization of soft electronic circuits without the need to directly contact the liquid metal itself. In particular, the semiconducting materials offer the possibility of establishing liquid metal-semiconducting junctions that can be used in the formation of novel electronic devices.

In liquid metal marble contacts, in addition to the properties of the semiconducting powder, which covers most of the surface of the liquid metal, the native oxide layer that is naturally formed on the surface and surrounding the rest of the liquid metal marble also plays an important role in the properties of the junction. In order to understand the electronic properties of liquid metal marbles coates with different types of powders and to assess the influence of the native metal oxide layer, eight different experiments were conducted. In these experiments, we investigated the effect of the native oxide layer and the characteristics of liquid metal marbles coated with n-type (WO_3) and p-type (CuO) semiconducting nanopowders in marble-metal and marble-marble configurations. Many other semiconducting powder materials were also investigated, however the results are not included for brevity.

Firstly, to demonstrate that it is possible to form an electrical interface across the n-type semiconducting coating (WO_3) without the native oxide layer on the surface of the liquid metal, we conducted the experiment in a nitrogen filled glove box at room temperature. We treated the liquid metal droplet with diluted HCl solution in the nitrogen glove box to ensure the native oxide was removed and then rolled the droplet on an 80 nm WO_3 powder bed to form the liquid metal marble. The marble was then placed onto a gold coated silicon wafer. We then inserted a probe electrode into the liquid metal marble and measured the current–voltage (I–V) characteristics of the electrical interface established from within the marble, across the particle coating and to the gold substrate. Four consecutive scans were performed measuring the current as the voltage was scanned from–9 V to +9 V. **Figure 5**a presents a photograph

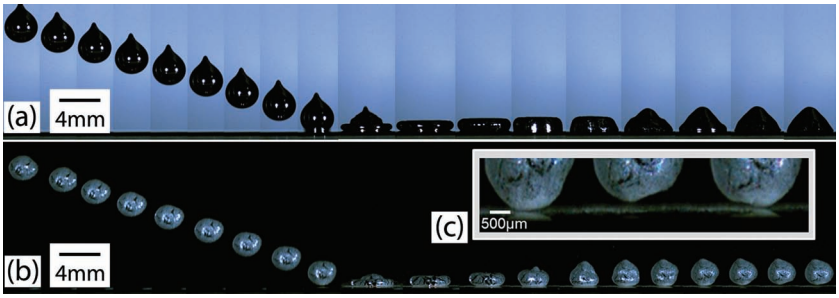

Figure 4. Successive snapshots of a) galinstan pendant drop and b) WO_3 coated galinstan liquid marble dropped from a height of 25 mm on a silicon wafer surface The time interval between two successive frames is 1.875 ms. c) Magnifications of the last three frames showing the bouncing of the galinstan liquid marble.

of the marble-metal configuration and also the measured *I–V* characteristics. The *I–V* characteristics are observed to be similar with consecutive voltage sweeps and there is no significant difference observed between subsequent sweeps.

The experiment was repeated on the same marble after being exposed to ambient air (including 21% oxygen). The obtain *I–V* characteristics are presented in Figure 5b. In this case, it can be observed that the current obtained for large and positive voltages slightly increased initially but then decreased after each subsequent voltage sweeps.

The next pair of experiments were conducted with two WO_3 coated marbles in contact resting on an insulating (Teflon) substrate (Figure 5c,d). In this pair, the first experiment was conducted with the galinstan droplets treated with diluted HCl solution before coating with WO_3 nanopowder in a nitrogen glove box. Electrodes were inserted into the liquid metal marbles and the *I–V* characteristics were recorded. Consecutive sweeps resulted in very similar responses as seen in Figure 5c. The experiment was then repeated on the same marbles after exposing them to to ambient air conditions. The *I–V* characteristics are presented in Figure 5d. In this case, the absolute current value obtained for both large negative and large positive voltages first increased but then significantly decreased with sequential voltage sweeps illustrating the significant impact that the formation of the native oxide layer had on the electronic properties of the liquid metal marbles.

The *I–V* characteristic behaviours in all cases of Figure 5 can be explained using well-established metal-semiconductor-metal (MSM) junction models.[27] It is suggested that the current transport behaviour of MSM junctions can be described using the thermo-ionic emission theory. The flow of current in such a junction is due to a combination of electron and hole carriers. In Figure 5, we observe that the curves are very much similar to that of a solid state MSM curve which is defined for an intermediate n–type semiconductor layer. The *I–V* curves can be divided into "three" separate stages, labelled in Figure 5 as I, II and III:

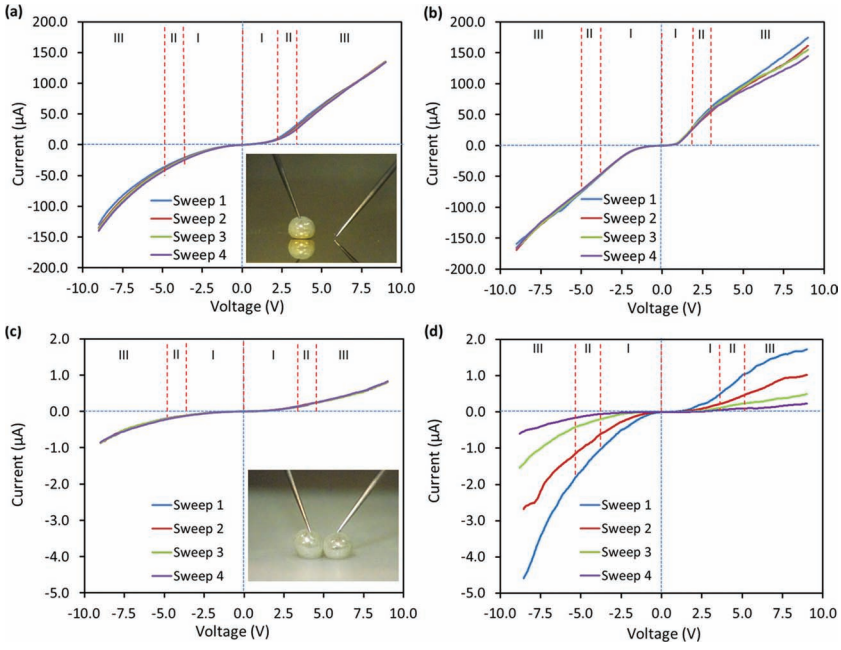

Figure 5. *I–V* characteristics of the WO_3 coated galinstan liquid marble - in contact with a gold substrate: a) in a nitrogen filled glove box to prevent oxidation, b) in ambient air condition; and c,d) in contact with another WO_3 coated galinstan liquid marble in a nitrogen filled glove box (c) and in ambient air condition (d). It is important to note that the same marbles were used for the experiment in the nitrogen filled glove box and in the ambient air condition measurements to allow the direct comparison of the *I–V* curves. The four consecutive voltage sweeps are labelled as sweeps 1, 2, 3, and 4.

In "Stage I", for small voltages (V), when the depletion regions of two metal-semiconductor (MS and SM) junctions do not coincide, which is called the reach-through voltage (V_{RT}), the main current density generated by the electron current is given by:

$$J_n \approx J_{ns} e^{\beta \Delta \phi n1} \left(1 - e^{-\beta V}\right), \; V < V_{RT} \tag{1}$$

Most of the voltage drops on the first junction, which is reverse biased, and is due to the saturation current (J_{ns}) and $\beta = q/kT$, in which k is the Boltzmann's constant, q is the charge of an electron and T is the temperature. $\Delta\phi_{n1}$ is the change in the barrier height, which is obtained using:

$$\Delta \phi_{n1} = \sqrt{\frac{q\,E}{4\pi\,\varepsilon_s}} \tag{2}$$

in which:

$$E = \sqrt{\frac{2q\,N_D}{\varepsilon_s}\,(V + V_D)} \tag{3}$$

where ε_s is the permittivity of the medium, N_D is the concentration of electrons per volume and V_D is the built in voltage.

In "Stage II", when the applied voltage is larger than the reach-through voltage and smaller than when the band becomes flat

(V_{FB}), the current density results from the combination of electron and hole carriers:

$$J \approx J_{ns} e^{\beta \Delta \phi n1} + J_{ps} \left[e^{-\frac{\beta (V - V_{FB})^2}{4(V_{FB})}} \right], \; V_{RT} < V < V_{FB} \quad (4)$$

in which J_{ps} is the saturation current for holes.

In "Stage III", when the applied voltages is greater than the flat-band voltage, the current density mostly results from the hole (minority) current:

$$J_p \approx J_{ps} e^{\beta \Delta \phi_{p2}}, \; V > V_{FB} \quad (5)$$

in which $\Delta \phi_{p2}$ is the change in the barrier height for the second junction.

The *I–V* curves demonstrated in Figure 5 can all be approximated by Equation (1) to (5) using different oxide layer thicknesses. As such, we ascribe the change in the *I–V* curve after the exposure to ambient air and sequential voltage sweeps to the changes of the oxide layer thickness as follows.

It can be observed that the *I–V* characteristics remained unchanged in the absence of the native oxide skin (in nitrogen environment) for both Figure 5a,c. It was expected to see a decrease of current after the exposure to the ambient air due to the formation of the native oxide. However, the opposite was observed. By comparing the *I–V* characteristics obtained in Figure 5a and the first sweep of the one in Figure 5b, we observed an increase in the maximum current in the experiment conducted in ambient air conditions. An explanation for this observation is given as follows. The nanopowder does not cover the whole surface of the metal droplet so there exists an air-gap. As a result, we suggest that this increase in maximum current is due to ionisation of the moisture laden gas species[28] in the air-gap which generates extra paths for the passage of current. In addition, the nanopowders have sharp edges and projections which also enhances the formation of plasma by augmenting the local electric field.[29] However, the existence of the ionic species generated by the plasma increase the thickness of the native oxide layer over time. As a result, the current decreases in the consecutive sweeps (Figure 5b). A similar observation can be made when comparing the *I–V* characteristics in Figure 5c,d. However, the decrease in current after the subsequent sweeps is much more prominent in this case. We ascribe this to the existence of the enhanced electric field by both sides of the contact that increase the rate of the oxidation and hence increasing the thickess of the native oxide formed. To test the role of ambient oxygen and moisture on the observed changes in *I–V* characteristics, we repeated the experiments with an acid treated marble in nitrogen, dry air and ambient air environments (Supporting Information S4). This clearly shows stable current under nitrogen; slowly diminishing current under dry air, due to oxidation; and a dramatic increase follow by rapid decrease in current under moisture laden ambient air, due to ionization and subsequent oxidation.

There are some significant differences between Figure 5a,c: Firstly, Stage II is shifted to the right side in the *I–V* curves for the two marbles (Figure 5b) which is caused by the prevalence of the second term in Equation (4) at lower voltages. Secondly, the current in the two marble case of Figure 5b is much smaller than for the single marble-metal case of Figure 5a. This is because the total thickness of the oxide layer increases in the case when two marbles are in contact, compared to the oxide layer thickness formed by a marble in contact with metal.

As a further investigation, we repeated the procedure used for obtaining the *I–V* characteristics of Figure 5, but incorporated a p-type semiconducting powder (CuO). **Figure 6**a,b present the *I–V* characteristics of a single p-type coated liquid metal marble contacting a metal substrate without and with the native oxide layer respectively; and Figure 6c,d present the characteristics of the marble-marble configuration without and with the native oxide layer respectively.

Similar to the case of the n-type materal (WO_3) shown in Figure 5, the *I–V* characteristics of the p-type material (CuO) coated marbles shown in Figure 6 also follows Equation (1) to (5) and calculations show that there is no significant changes in the form of the *I–V* curves, which is as expected due to nature of the MSM contacts. The observed overall current is significantly lower for the contacts made of CuO particle coatings, which can be explained due to the smaller electrical conductivity of as-purchased CuO particles compared to that of WO_3 particles (measured WO_3 conductivity was approximately three times larger than CuO).

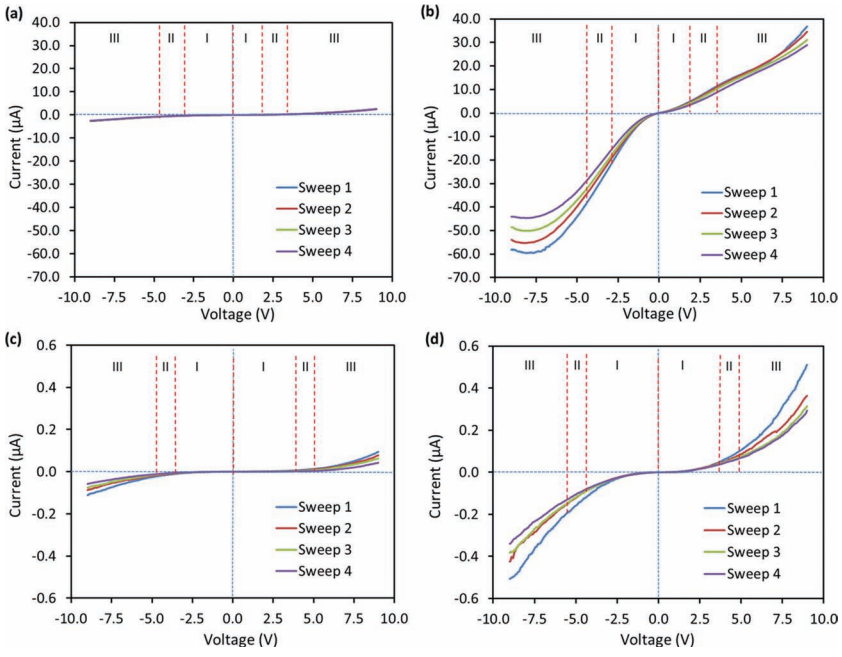

Figure 6. *I–V* characteristics of the CuO coated galinstan liquid marble - in contact with a gold substrate: a) in a nitrogen filled glove box to prevent the formation of a native oxide layer, b) in ambient air condition; and c,d) in contact with another CuO coated galinstan liquid marble in a nitrogen filled glove box (c) to prevent the formation of a native oxide layer and in ambient air condition (d). The four consecutive voltage sweeps are labelled as sweep 1, 2, 3, and 4.

These preliminary results indicate that it is possible to form simple circuits using these liquid metal marbles and crudely covered semiconducting nano-particles coatings. It is possible to form many other types of junctions including metal/p-type semiconductor/n-type semiconductor/metal junctions with interesting *I–V* characteristics. However, this investigation is beyond the scope of this paper.

5. Electrochemical Properties

As a final demonstration of the utility of these liquid metal marbles, we investigate their use for heavy metal ion sensing. Galinstan has been used as a heavy metal ion sensing material and has been shown as an attractive alternative to mercury, possessing a high hydrogen over-potential, predictable electrochemical behaviour and simple surface renewal in properties, which allows high reproducibility, and the non-toxicity of this alloy.[24] Here, we show that it is possible to dramatically enhance the sensitivity by coating the liquid metal with semiconducting nanoparticles.

We used a hanging galinstan drop electrode (HGDE) configuration similar to that previously reported,[20] and compare this to the situation where the liquid metal droplet is coated with WO_3 nanoparticles. In this investigation we used emersion in a colloidal suspension of 80 nm WO_3 nanoparticles to form the coating. Four different cases were studied, uncoated galinstan and galinstan immersed in suspensions of 0.1 g, 0.4 g and 0.7 g of WO_3 per 50 ml of DI water to achieve an increased amount of WO_3 dispersed over the surface of the galinstan marble as shown in Supporting Information S1. A schematic of the experimental setup is shown in **Figure 7**a. The HGDE, auxillary graphite and reference electrodes were immersed in an electrolyte containing both Pb and Cd ions and differential pulse voltammetry was performed.

Figure 7b presents the differential pulse voltammogram of Pb^{2+} and Cd^{2+} in an acetate buffer solution. We observe selectivity for Pb and Cd ions that are present in the solution. We also observe an enhancement in the sensitivity for detection of the metal ions on the coated marbles when compared to that of the uncoated galinstan droplet. To aid comparision, the response obtained for the sensing of Pb ions of the uncoated droplet is magnified in Figure 7c showing that the response of the coated marbles is much stronger than the uncoated droplet. The particle density on the surface influences the enhancement. A further observation is that the current peaks appear to be shifted to a lower potential in the case of coated liquid metal electrodes. This can be explained due to the barrier potential of the semiconducting WO_3 and is a desirable effect since it expands the negative potential window for heavy metal ion sensing.

At pH 6.0 and over the voltage range employed, electrochemical reduction of the native oxide layer that is normally formed in ambient air condition on the surface of this liquid metal would be expected.[30] There is also a significant shift in the onset potential to less negative values and increase in current magnitude for the reduction of Pb ions onto the galinstan surface when coated with WO_3 particles. The response is also sharper when compared to the unmodified surface. The possibility of a change in the surface area of galinstan or the diffusion of Pb^{2+} ions to the electrode surface accounting for this was investigated by coating the galinstan drop with non-conductive particles such as Teflon (Supporting Information S5). No significant enhancement in current or change in onset potential was observed. This indicates that there is a large reduction in the overpotential required for the reduction of Pb^{2+} to Pb^0 on the WO_3 modified surface and possibly more facile amalgamation of Pb^0 with galinstan. The creation of a triple phase galinstan/WO_3/electrolyte region may be crucial in creating hot spots, where the transfer of electrons is facilitated as observed in many nanostructured electrode studies. The magnitude of the

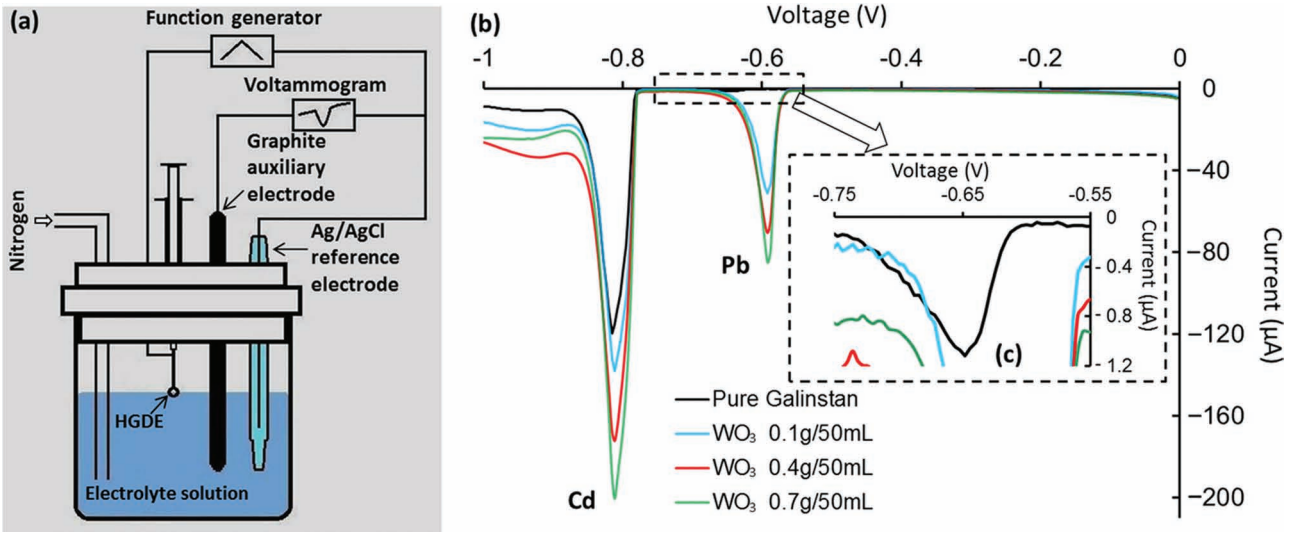

Figure 7. a) Schematic of the experimental setup using HGDE for heavy metal ion sensing application. b) Differential pulse voltammogram (DPV) of Pb^{2+} (10 mmol/L) and Cd^{2+} (10 mmol/L), obtained with HGDE coated with WO_3 nano-powder using the submerging technique with the nanoparticles dispersed in DI water having concentrations of 0.1 g in 50 ml, 0.4 g in 50 ml and 0.7 g in 50 ml at pH = 6.0. c) A magnified plot of the response of the DPV sensing Pb^{2+} ions using galinstan in the HGDE.

response increases with an increased loading of WO_3 on the galinstan surface (the effect of increased WO_3 solution concentration on loading of the surface of galinstan can be observed in the Supporting Information S1).

We repeated the experiment of Figure 7 with a liquid metal marble formed by rolling a galinstan droplet over a WO_3 powder bed to form a dense multi-layer WO_3 coating (Supporting Information S6). When the surface coverage of WO_3 is significantly increased there is a large increase in the reduction current and a new process at ca. –0.40 V, which is significantly reduced during subsequent voltage sweeps. The latter may be attributed to the intercalation of electrolyte cations into WO_3 as indicated by the change in color of the sample in this potential range (Supporting Information S7). This process was also observed to occur in the absence of Pb^{2+} ions. This is followed by a large increase in cathodic current at –0.90V until the end of the sweep which is due to the hydrogen evolution reaction at WO_3.

From a practical viewpoint, this composite shows promise in that not only the sensitivity for heavy metal detection is increased as observed for Pb^{2+} detection but it also demonstrates selectivity as in the case of unmodified galinstan whereby Cd^{2+} ions were detected at a distinctly more negative potential of ca. –0.80 V. Interestingly in the latter case there is no shift in the onset potential for the reduction of Cd^{2+} to Cd^0 at the modified galinstan electrode but there is a significant increase in the current magnitude. This indicates that the electron transfer process for the reduction of Cd^{2+} ions to Cd^0 or amalgamation of Cd with galinstan is not influenced to the same extent as observed in the case of Pb. However the presence of the initially formed Pb in the galinstan may be accountable for this observation. These measurements were repeatable on different similarly sized and coated marbles (Supporting Information S8)

6. Discussion and Conclusions

We have introduced liquid metal marbles formed from droplets of the liquid metal galinstan coated with insulators and semiconductors. We have demonstrated some of the unique physical, electronic and electrochemical properties of these liquid metal marbles. We demonstrated that physically there are similarities and differences between conventional liquid marbles and liquid metal marbles. High surface tension, the formation of a native oxide and high density of liquid metal marbles are the properties that give them their extraordinary physical features. Electronic properties of liquid metal marbles were characterized and metal-semiconductor-metal junction behaviour was observed which can be extended into many applications in soft electronic devices. It was also shown that the nanoparticle coated liquid metal marbles can provide enhanced sensing of heavy metals, presenting a new avenue for investigation into safe and highly sensitive systems for the detection of low concentrations of heavy metal ions with high selectivity.

There are many other possible applications that can be considered. For instance, the coatings provide a non-stick property to the liquid metal marbles and hence can be used as conductive lubricants. They should operate much better than the conventional liquid marbles in tolerating heavy load and pressure as their surface tension is much higher. The high evaporation point and low vapor pressure of liquid metal marbles can be some of the unique properties allowing them to operate at very high temperatures as well as in a vacuum. Conventional liquid marbles can be made conductive, but only through use of ionic liquids which are very poor subsitutes for traditional electrodes. Conversely, liquid metal marbles have conductivities approaching solid metals and can be coated with a wide variety of both insulating and of semiconducting materials enabling many different circuit elements, including diodes and transistors, that could be considered for soft electronic circuits. These preliminary demonstrations certainly illustrate promise of what this new approach to the use of liquid metals as liquid metal marbles can offer for future scientific research and technological applications.

7. Experimental Section

Realization of Liquid Metal Marbles: Galinstan (Geratherm Medical AG, Geschwenda, Germany) was used to realise the liquid metal marble. Two different approaches are presented in this work. Method 1: A droplet of galinstan was dispensed through a syringe on a powder bed and rolled until the entire surface of the droplet was covered by the powder material. Different powder materials including WO_3, In_2O_3, ZnO, Al_2O_3 and TiO_2 purchased from China Rare Ltd.; CuO and Teflon from Sigma Adrich; and carbon nanotubes from CheapTubes Ltd. were used. Method 2: A colloidal solution of nano size powder was formed by dispensing a specific quantity of a powder material in de-ionised (DI) water (50 ml) and dispersing it using a high intensity ultrasonic processor (GEX500) for 30 min. A droplet of galinstan is then submerged into the colloidal solution for 5 s.

Characterization: SEM images were taken using a FEI Nova NanoSEM. The contact angles were measured using a Dataphysics OCA20 contact angle measuring system at ambient temperature. High speed imaging of the free fall and impact images and films were taken using a high-speed video camera (Phantom v4.3, Vision Research Inc.) fitted with a Navitar 12mm Zoom 6000 lens, 0.67× adapter, and 0.25× lens attachment. Events were captured at 1600 frames per second, with a resolution of 608 pixels × 600 pixels and an exposure time of 248 µs for each frame.

Electronic Properties: For investigating the electrical characteristics of liquid metal marbles, the *I–V* characteristic curves were obtained by using a Lab-view controlled source meter (Keithley 2602, Keithley Instruments Inc.). Tungsten probes attached to micromanipulators were employed to connect with the liquid metal marbles and the gold coated substrates for the different electrical measurements.

Electrochemical Properties: For heavy metal ion sensing, all measurements were performed using a CH Instruments (CHI 413A) electrochemical analyser. The reference electrode was Ag/AgCl (aqueous 3 M KCl) and an inert graphite rod (3 mm diameter, Johnson Matthey Ultra "F" purity grade) was used as the auxiliary electrode, based on the three–electrode configuration for the electrochemical measurements. All chemicals were of analytical grade purity and all aqueous solutions were prepared using Milli–Q water. All electrochemical measurements commenced after degassing the electrolyte solutions with nitrogen for at least 10 min prior to any measurement. Acetate buffer solutions with a pH of 6.0 were used as the supporting electrolyte, which was prepared by dissolving a sample of ammonium acetate (33.33 g) from Ajax Finechem in Milli–Q water (100 mL). The pH was corrected by adding acetic acid (99.7%, Ajax Finechem) and measured using a microprocessor controlled pH meter (PH 213, HANNA Instruments). Lead ions (Pb^{2+}) and cadmium ions (Cd^{2+}) were incorporated in the supporting electrolyte by dissolving lead (II) acetate 3–hydrate (BDH, AnalaR) and cadmium (II) nitride 4–hydrate (Ajax Finechem). The methodology adopted for

the electrochemical measurements was differential pulse polarography (DPP) with a pulse amplitude of –50 mV and a pulse period of 0.5 s.

Supporting Information

Supporting Information is available from the Wiley Online Library or from the author.

Acknowledgements

The authors acknowledge the facilities, and the scientific and technical assistance, of the Australian Microscopy & Microanalysis Research Facility at the RMIT Microscopy & Microanalysis Facility, at RMIT University.

Received: March 25, 2012
Revised: May 21, 2012
Published online: August 7, 2012

[1] P. Aussillous, D. Quéré, *Nature* **2001**, *411*, 924.
[2] P. Aussillous, D. Quéré, *Proc. R. Soc. A.* **2006**, *462*, 973.
[3] E. Bormashenko, Y. Bormashenko, A. Musin, *J. Colloid Interface Sci.* **2009**, *333*, 419.
[4] E. Bormashenko, Y. Bormashenko, A. Musin, Z. Barkay, *ChemPhysChem* **2009**, *10*, 654.
[5] L. Gao, T. J. McCarthy, *Langmuir* **2007**, *23*, 10445.
[6] A. Venkateswara Rao, M. M. Kulkarni, S. D. Bhagat, *J. Colloid Interface Sci.* **2005**, *285*, 413.
[7] T. Arbatan, L. Li, J. Tian, W. Shen, *Adv. Healthcare Mater.* **2012**, *1*, 80.
[8] N. Eshtiaghi, K. P. Hapgood, *Powder Technol.* **2012**, *223*, 65.
[9] T. Arbatan, W. Shen, *Langmuir* **2011**, *27*, 12923.
[10] E. Bormashenko, *Curr. Opin. Colloid Interface Sci.* **2011**, *16*, 266.
[11] P. Sen, K. Chang-Jin, *IEEE Trans. Ind. Electron.* **2009**, *56*, 1314.
[12] H. J. Koo, J. H. So, M. D. Dickey, O. D. Velev, *Adv. Mater.* **2011**, *23*, 3559.
[13] J. H. So, H. J. Koo, M. D. Dickey, O. D. Velev, *Adv. Funct. Mater.* **2012**, *22*, 625.
[14] L. Tingyi, P. Sen, K. Chang-Jin, *J. Microelectromech. Sys.* **2012**, *21*, 443.
[15] B. L. Mellor, N. A. Kellis, B. A. Mazzeo, *Rev. Sci. Instrum.* **2011**, *82*, 046110.
[16] S. Cheng, A. Rydberg, K. Hjort, Z. Wu, *Appl. Phys. Lett.* **2009**, *94*, 144103.
[17] M. Kubo, X. Li, C. Kim, M. Hashimoto, B. J. Wiley, D. Ham, G. M. Whitesides, *Adv. Mater.* **2010**, *22*, 2749.
[18] J. H. So, J. Thelen, A. Qusba, G. J. Hayes, G. Lazzi, M. D. Dickey, *Adv. Funct. Mater.* **2009**, *19*, 3632.
[19] K. Hyun-Joong, T. Maleki, W. Pinghung, B. Ziaie, *J. Microelectromech. Sys.* **2009**, *18*, 138.
[20] H. J. Kim, C. Son, B. Ziaie, *Appl. Phys. Lett.* **2008**, *92*, 011904.
[21] A. C. Siegel, S. S. Shevkoplyas, D. B. Weibel, D. A. Bruzewicz, A. W. Martinez, G. M. Whitesides, *Angew. Chem. Int. Ed.* **2006**, *45*, 6877.
[22] C. Chung-Hao, J. Whalen, D. Peroulis, *IEEE MTT-S Int. Microwave Symp. Dig. Jun* **2007**, 363.
[23] M. R. Khan, G. J. Hayes, J.-H. So, G. Lazzi, M. D. Dickey, *Appl. Phys. Lett.* **2011**, *99*, 013501.
[24] P. Surmann, H. Zeyat, *Anal. Bioanal.Chem.* **2005**, *383*, 1009.
[25] R. G. Burton, R. A. Burton, *IEEE Trans. Compon., Hybrids, Manuf. Technol.* **1988**, *11*, 112.
[26] V. Kocourek, C. Karcher, M. Conrath, D. Schulze, *Phys. Rev. E: Stat., Nonlinear, Soft. Matter Phys.* **2006**, *74*, 026303.
[27] S. M. Sze, D. J. Coleman Jr, A. Loya, *Solid State Electron.* **1971**, *14*, 1209.
[28] M. Pavlik, J. D. Skalny, *Rapid Commun. Mass Spectrom.* **1997**, *11*, 1757.
[29] J. Yu, M. Shafiei, W. Wlodarski, Y. X. Li, K. Kalantar-zadeh, *J. Phys. D: Appl. Phys.* **2010**, *43*, 025103.
[30] J. H. So, M. D. Dickey, *Lab Chip* **2011**, *11*, 905.